

Document Version

Final published version

Licence

CC BY

Citation (APA)

Hendrickx, G. G., Fivash, G. S., Gerritsma, A., Geraeds, M., & Pearson, S. G. (2026). Socio-ecological evaluation of estuary-scale interventions: Case study of reopening the Haringvliet, the Netherlands. *Ecological Engineering*, 230, Article 108031. <https://doi.org/10.1016/j.ecoleng.2026.108031>

Important note

To cite this publication, please use the final published version (if applicable).
Please check the document version above.

Copyright

In case the licence states "Dutch Copyright Act (Article 25fa)", this publication was made available Green Open Access via the TU Delft Institutional Repository pursuant to Dutch Copyright Act (Article 25fa, the Taverne amendment). This provision does not affect copyright ownership.
Unless copyright is transferred by contract or statute, it remains with the copyright holder.

Sharing and reuse

Other than for strictly personal use, it is not permitted to download, forward or distribute the text or part of it, without the consent of the author(s) and/or copyright holder(s), unless the work is under an open content license such as Creative Commons.

Takedown policy

Please contact us and provide details if you believe this document breaches copyrights.
We will remove access to the work immediately and investigate your claim.



Socio-ecological evaluation of estuary-scale interventions: Case study of reopening the Haringvliet, the Netherlands

Gijs G. Hendrickx^{a,b}, Gregory S. Fivash^c, Avelon Gerritsma^d, Marlein Geraeds^a,
Stuart G. Pearson^a,*

^a Department of Hydraulic Engineering, Delft University of Technology, Delft, the Netherlands

^b Department of Rivers, Coasts, and Deltas, HKV lijn in water, Lelystad, the Netherlands

^c Department of Biology, University of Antwerp, Antwerp, Belgium

^d Department of Mathematical Physics, Delft University of Technology, Delft, the Netherlands

ARTICLE INFO

Keywords:

Estuaries
Nature-based solutions
Ecotopes
Physiotopes
Salt intrusion
Haringvliet

ABSTRACT

Estuaries are considered valuable regions, both socio-economically and ecologically. The gradients in physical characteristics like salinity present result in a high biodiversity, while the provision of many ecosystem services have attracted human settlement and activity. Human activities and estuarine biodiversity are often at odds with each other, leading to socio-ecological trade-offs in decision- and policy-making in which the ecological perspective is generally underrepresented. In this study, we implemented a hydrodynamic model to explore the socio-ecological implications of reopening the closed-off Haringvliet estuary in the Netherlands. Our socio-ecological evaluation considers the trade-off between freshwater availability and ecological diversity. In the case of the Haringvliet, we have shown that partially opening the gates enhances diversity in the system against no — or limited — loss of freshwater availability. All in all, the use of representative (non-monetary) performance indicators for the considered stakeholders allowed us to demonstrate the trade-offs in a clear fashion: the Pareto-front resulting from these performance indicators is an intuitive visualization for decision- and policy-makers as well as the communication to the public.

1. Introduction

At the interface between freshwater river systems and the saline ocean waters, estuaries are valuable regions, both socio-economically and ecologically. Estuaries provide a multitude of natural and ecosystem services (Barbier et al., 2011; Worm et al., 2006), e.g., low-dynamic regions within an estuary are often used as nurseries (Breine et al., 2011; Tulp et al., 2008). Due to the multitude of gradients present in estuaries, such as salinity, they experience a high biodiversity (Mestdagh et al., 2020; Tangelder et al., 2017; Ysebaert et al., 2003) despite the minimum in number of species thriving in brackish waters (Cloern et al., 2017; Remane, 1934; Whitfield et al., 2012).

In addition, coastal and estuarine regions are densely populated by humans, and these populations are expected to densify in the future (Maul and Duedall, 2019; Neumann et al., 2015). In these regions, the natural dynamics largely dictate the provision of crucial functions; examples include (1) freshwater availability, which is susceptible to salt contamination due to the near-by saline seawater (e.g., Bakker et al., 2025; Costa et al., 2023; Jones et al., 2023); and (2) safety against

flooding by natural sheltering and wave damping (e.g., Fairchild et al., 2021; Temmerman et al., 2013).

In an attempt to control the provision of these crucial functions, human interventions have had major impacts on estuarine systems (e.g., van Wesenbeeck et al., 2014; Yang et al., 2010). These interventions range from dredging activities to maintain naval transportation routes (van Dijk et al., 2021; de Vriend et al., 2011) to completely damming off estuaries for flood safety and/or freshwater availability (Figuroa et al., 2022; Orton et al., 2023; Tönis et al., 2002). Human interventions are the product of weighing a multitude of — often conflicting — objectives, such as freshwater availability versus port accessibility (Bakker et al., 2025).

However, the ecological consequences of such interventions are rarely considered in a similar manner (e.g., Bice et al., 2023; van Wesenbeeck et al., 2014), weighing the costs and benefits against each other. This is in part due to the conflicting interests within the ecological system itself (Bice et al., 2023): The displacement of one habitat generally results in the creation of another. Therefore, weighing various ecological states inherently requires a subjective value

* Corresponding author.

E-mail address: S.G.Pearson@tudelft.nl (S.G. Pearson).

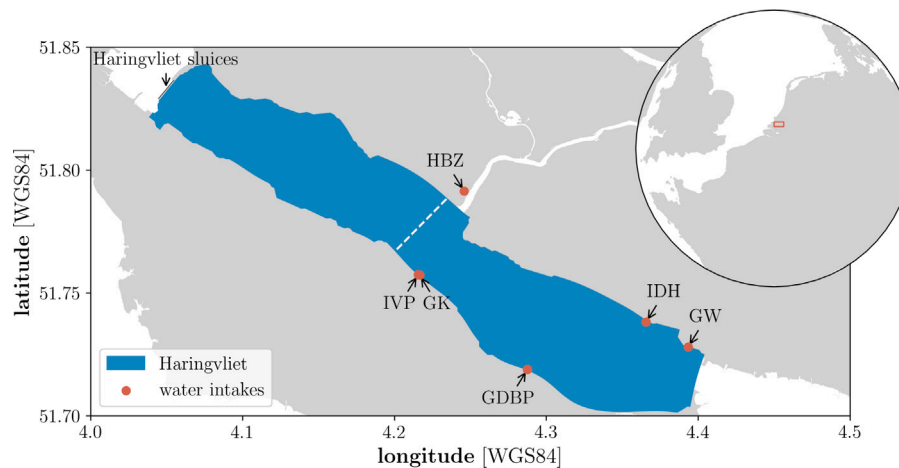


Fig. 1. Haringvliet in the south west of the Netherlands, including the Haringvliet sluices and water intake locations (Table 3 for abbreviations). The white, dashed line indicates the “Middelharnis-Spui line”. (For interpretation of the references to colour in this figure legend, the reader is referred to the web version of this article.)

judgement. Nevertheless, large-scale interventions — such as (partially) closing off an estuary — have tremendous implications for the ecological system (Smaal and Nienhuis, 1992; Yang et al., 2010), and the ecosystem services provided by the area of interest.

One such closed-off estuary is the Haringvliet, located in the south-west of the Netherlands (Fig. 1). Since 1970, the Haringvliet is a semi-closed, freshwater system due to the construction of the Haringvliet sluices, which are part of the Delta Works. Prior to construction, the Haringvliet was an estuary in which the tidal range and salinity reached 50 kilometres landward (Bol and Kraak, 1998; Tönis et al., 2002). Closing off the Haringvliet estuary with sluices that are opened only to release excess river discharge has improved flood safety as well as freshwater availability. However, this has been at the expense of removing a rare brackish, estuarine ecosystem (Tangelder et al., 2017). In addition, the Haringvliet sluices also removed the connectivity between the North Sea and the Rhine-Meuse river system, limiting fish migration between the river system and the sea (Beeldman et al., 2018; Hop and Vriese, 2011).

Recently, experiments with partially opening the gates during flood have been initiated to restore fish migration in this area with the so-called “Kierbesluit” (*trans.*: “Ajar policy”; Brevé et al., 2019; de la Haye et al., 2022). To ensure freshwater availability, a line was drawn between Middelharnis and Spui beyond which no saline influence was allowed, as all water intakes in the Haringvliet are east of this “Middelharnis-Spui line” (Fig. 1). As the bathymetry of the Haringvliet still resembles that of an active estuary with deep pits, opening the Haringvliet sluices — albeit slightly — can threaten the availability of freshwater in the region by up-stirring of saline water that accumulates in these deep pits (Kranenburg et al., 2023).

The case of the Haringvliet is a prime example of a trade-off between ecological impacts and natural resource availability: how to find a balance between these opposing goals? In past decades, much emphasis has been placed on the quantification and valuation of ecosystem services (e.g., Barbier et al., 2011; Granek et al., 2010; Heimhuber et al., 2024; Worm et al., 2006). However, the valuation of ecosystem services requires know-how about the ecosystems and how they will develop (Liquete et al., 2013), which is by no means trivial. The use of ecotopes as an intermediate step as been shown valuable and extendable across regions, from Belgium (Radoux et al., 2019), the United States of America (del Moral and Fleming, 1980), to South Africa (Mzezewa et al., 2010), and China (Ye et al., 2016). Such a classification system based on ecotopes is considered as ecologically valuable (Galván et al., 2021; Muller et al., 2020), especially if it can be incorporated in modelling studies instead of relying on *in-situ* data (Brunink and Hendrickx, 2024).

Furthermore, assessments using ecosystem services strongly focus on economic gains (Barbier et al., 2011; Liquete et al., 2013), such as the fishing industry (Heimhuber et al., 2024). This leads to other values of ecosystem services to be underrepresented, such as ecologically valuable habitats.

Hence, the aim of this paper is to provide a method to compare socio-ecological objectives in an estuarine system in which ecological objectives are accounted for, aiding decision- and policy-makers. In this way, we address the research question of how decision- and policy-makers could incorporate ecological impacts due to system modifications. By quantifying the ecological impacts of interventions, we seek to provide new insights for the management and/or restoration of estuarine systems. As a case study, we use the Haringvliet in which current policy-making is concerned with such a socio-ecological trade-off.

2. Method

In this study, we used the Haringvliet as a case study in which the gates of the Haringvliet sluices were opened at different heights. At the basis, we used a hydrodynamic model of the Rhine-Meuse Delta, which is presented in Section 2.1. The implications of opening the gates were assessed by means of (1) ecological diversity (Section 2.2), and (2) freshwater availability (Section 2.3).

2.1. Hydrodynamic model

This study executed model simulations using the hydrodynamic modelling software Delft3D Flexible Mesh (Kernkamp et al., 2011). This software is used to solve the Reynolds-averaged Navier–Stokes equations, assuming hydrostatic pressure and implementing the $k-\epsilon$ turbulence closure model.

The “RMD model” is a hydrodynamic model of the Rhine-Meuse Delta (Geraeds et al., *in review*; Gerritsma et al., 2025), which includes the Haringvliet. The model domain extends 35 km offshore of the Dutch coastline, where the grid resolution is $600 \times 1,200$ m, and refines towards the coastline to become 170×290 m. The river branches laterally span at least eight grid cells (20 m each), and depending on the river branch have a length of 60–100 m. In the Haringvliet, the cell size is approximately 135×75 m, and the Haringvliet sluices are included as operable structures.

We implemented a combined Z, σ -layering for the vertical discretization: the top layers were defined as σ -layers that follow the temporal fluctuations of the water level, and the bottom layers maintain

Table 1

Overview of simulations. z_g is the height of the gates with respect to the bottom (i.e., $z = -5.50$ m NAP); and A_g is the flow area through the sluices, i.e., $A_g = z_g W_g$ with $W_g = 992.5$ m. The simulation “reference” represents the time-dependent opening regime as applied in 2019, which includes the “Kierbesluit” adaptation; and “open” represents the situation as if the gates have been removed from the Haringvliet sluices entirely.

Description	z_g [m]	A_g [m ²]
reference	$z_g(t)$	$A_g(t)$
closed	0.00	0
	0.50	496
partial	1.50	1489
	2.10	2084
	2.75	2729
open	∞	∞

a constant cell thickness — so-called *Z*-layers — to better represent salt dynamics (Stelling and van Kester, 1994). There are nine *Z*-layers atop the *Z*-layers, which have a constant thickness of $\Delta z = 0.75$ m down to $z = -15$ m below which the thickness of the *Z*-layers grows by a factor of 1.15. A more detailed description of the RMD model can be found in Gerritsma et al. (2025).

The RMD model is executed for the year 2019, which has been extensively calibrated and validated by Geraeds et al. (in review). The skill of the model shows high correlation coefficients (r) between simulation and measurement: for water levels, $r \geq 0.95$; and for salinity, $r \approx 0.8$. The RMD model performs slightly less regarding salinity in the Haringvliet — our area of interest — with a representative value of $r = 0.67$; performances of the model regarding water levels in the Haringvliet are comparable with the rest of the Rhine-Meuse Delta: $r = 0.95$.

In the reference simulation, the opening and closing of the Haringvliet sluices were based on water levels at both sides of the structure and represent the implementation of the “Kierbesluit”. For the other simulations, we applied a fixed level of the gates, i.e., a fixed flow area between the North Sea and the Haringvliet. All gates are completely closed when reaching $z = -5.50$ m NAP, and are 58.5 m wide — except for the outermost gates, which are 57.5 m wide — totalling to an opening width of $W_g = 992.5$ m. In addition to completely closing and opening of the Haringvliet sluices, we have also included intermediate opening levels of the gates—all within the feasible range of the structure.

The height of the gates is notated as z_g , which is taken with respect to the bottom of the gates—i.e., $z_g = 0.00$ m for $z = -5.50$ m NAP. In all simulations, we have implemented a constant height of the gates, except for the reference case representing the “Kierbesluit”, which implements a time-varying height—i.e., $z_g = z_g(t)$. An overview of the simulations is presented in Table 1.

2.2. Ecological metric

In order to evaluate the ecological implications of opening/closing the Haringvliet sluices, we used EMMA (Ecotope-Map Maker based on Abiotics; Brunink and Hendrickx, 2024). EMMA determines which ecotope is most likely to occupy an area based on the prevailing abiotic characteristics (based on Bouma et al., 2005; Parea, 2021); these include three hydrodynamic variables that can readily be extracted from most hydrodynamic models: (1) water depth; (2) flow velocity; and (3) salinity. EMMA translates these three hydrodynamic variables to ecotope codes (Table 2), where we only consider soft substratum and limit the level of detail until which EMMA performs well (performance of 73.5% for listed classes in Table 2; Brunink and Hendrickx, 2024).

For this study, we implemented a small change to EMMA compared to Brunink and Hendrickx (2024) regarding the freshwater ecotopes: Areas with the yearly average of the tidal maximum salinity levels below 0.27 psu were labelled as *freshwater* ecotopes, regardless of the

Table 2

Meaning of ecotope-codes as used in EMMA. The ecotope-code is built-up as ab.cd with a the salinity label, b the substratum label, c the depth label, and d the hydrodynamics label. μ_s and σ_s are the annual mean and standard deviation of the depth-averaged, tidal salinity maxima [psu]; z_b is the bed level [m]; MLWS is mean-low-water-spring [m]; MHWN is mean-high-water-neap [m]; and μ_u is the annual mean of the tidal flow velocity maxima [ms⁻¹].

Class	Label	Meaning	Definition	
a	salinity	Z	marine	$\mu_s > 18$ psu ^a
		B	brackish	$5.4 \leq \mu_s \leq 18$ psu ^a
		F	freshwater	$\mu_s < 5.4$ psu ^a
		V	variable	$\mu_s < 4\sigma_s$
b	substratum	1	hard substratum ^b	
		2	soft substratum	
c	depth	1	sub-littoral	$z_b < \text{MLWS}$
		2	littoral	$\text{MLWS} \leq z_b \leq \text{MHWN}$
		3	supra-littoral	$z_b > \text{MHWN}$
d	hydrodynamics	1	high-energy	$\mu_u > 0.7$ ms ⁻¹
		2	low-energy	$\mu_u \leq 0.7$ ms ⁻¹
		3	stagnant	$\mu_u = 0.0$ ms ⁻¹

^a These thresholds are overruled when the variable classification applies (i.e., $\mu_s < 4\sigma_s$), except for $\mu_s \leq 0.27$ psu being freshwater (see text).

^b The hard substratum is included here for completeness, as this study only considers the soft substratum.

variability in the tidal maximum salinity levels. This threshold follows from the drinking water criteria in the Netherlands (Section 2.3). This small adaptation corrects the sensitivity to negligible fluctuations in salinity when the mean salinity is near zero.

The ecotope maps generated with EMMA were assessed in two manners: (1) the diversity of ecotopes; and (2) the change in ecotope area. In the first assessment, we used a simplified diversity metric — the Shannon index (Shannon, 1948) — to quantify the ecological richness of various model scenarios. The latter provided a more holistic view of the ecological impact, reflecting on three ecological aspects: (1) which ecotopes are present in the Haringvliet; (2) how much (relative) area do these ecotopes cover; and (3) how would the distribution of ecotopes transition between alternatives.

The Shannon index is originally a quantification of information (Shannon, 1948) and has often been used as a metric to quantify the biodiversity of an ecosystem (e.g., Kubicek et al., 2019; Medeiros et al., 2012; Smith et al., 2023). Here, we used the index to quantify the diversity of the ecotopes, i.e., ecotope diversity (based on Shannon, 1948):

$$H' = - \sum_i^N p_i \ln p_i \quad (1)$$

where N is the number of ecotopes [–]; and p_i the area fraction of ecotope i [–], such that $\sum_i^N p_i = 1$.

From Eq. (1), we can derive the evenness-index (Pielou, 1966), which we used as ecological performance indicator:

$$P_e = \frac{H'}{\ln N} \in [0, 1] \quad (2)$$

Note that at the level of detail considered, there are 36 possible ecotopes (i.e., $N = 36$), which follows from the number of combinations possible with the labels in Table 2 with only soft substratum (i.e., $b = 2$).

The diversity in the form of the Shannon index (Eq. (1)) was used as the basis of a single-value metric due to its close relation to ecosystem services (Hooper et al., 2005; Loreau et al., 2001; Worm et al., 2006), which are frequently used in assessing nature-based solutions (e.g., Barbier et al., 2011; Granek et al., 2010; Heimhuber et al., 2024). Furthermore, diversity is linked to ecological functioning, ecosystem resilience, and adaptability to changing environmental conditions (e.g., Elmqvist et al., 2003; Limberger et al., 2023; Loreau et al., 2001; Yachi

and Loreau, 1999). Diversity at the landscape-level — i.e., ecotope diversity — especially contributes to the resilience of an ecosystem (Folke et al., 2002; Loreau et al., 2003; Vasiliev, 2022). Hence, ecotope diversity enhances ecosystem resilience. Note, however, that such a single-value metric may facilitate “metric fixation” (Muller, 2021): the undesired single-minded focus on a metric without consideration of the complexity left-out.

Therefore, the ecotope maps were also presented as a barcode, showing the areal distribution of ecotopes in the area of interest, i.e., the p_i -values of a given system-state (e.g., Fig. 5). This ecotope barcode representation is similar to Timmerman et al. (2021), except that our barcode represents the whole area of interest instead of a single transect.

2.3. Socio-economic metric

The socio-economic metric was related to the freshwater availability in a similar fashion as in Bakker et al. (2025): The operations of the water intakes reflect the interests of the inhabitants, agricultural sector, and industry. The water intakes withdraw freshwater based on free-flow, i.e., the water level outside must exceed a threshold water level for the water to flow into the intake by gravity. In the Netherlands, the salinity of the water is not allowed to exceed the critical threshold of $s_c = 150 \text{ mg Cl}^- \text{ l}^{-1}$ (or 0.27 psu). Thus, water extraction only occurs if the following two criteria are met:

$$\eta(t) > \eta_c \quad (3a)$$

$$s(t) < s_c \quad (3b)$$

where η is the water level [m]; s the salinity [psu]; and the subscript c reflects the critical threshold.

Due to fluctuations in supply and demand of freshwater, freshwater storage volumes are present in the water board’s water systems, and so were incorporated in this study. Such storage functioned as the control volume in the freshwater mass balance:

$$\frac{dV}{dt} = E(\eta, s) - D(t) \quad (4)$$

where V is the freshwater storage volume [m^3]; E the extraction rate (Eq. (5)) [m^3s^{-1}]; and D the freshwater demand [m^3s^{-1}].

The supply of freshwater followed a binary signal, based on whether the extraction criteria were met (i.e., Eqs. (3a) and (3b)):

$$E = \begin{cases} E_{\max} & \text{if Eqs. (3a) and (3b)} \\ 0 & \text{else} \end{cases} \quad (5)$$

where E_{\max} is the maximum extraction rate of a water intake [m^3s^{-1}].

The freshwater storage in Eq. (4) cannot become negative, and is capped by a storage capacity:

$$0 \leq V \leq V_c \quad (6)$$

where V_c is the freshwater storage capacity [m^3].

From this mass balance, we defined water shortage as the demand that cannot be met. This means that the demand exceeds the extraction rate ($D > E$), while the freshwater storage cannot cover the deficit ($V < D - E$):

$$S = \begin{cases} D - E - \max\left\{-\frac{dV}{dt}; 0\right\} & \text{if } V < D - E \\ 0 & \text{else} \end{cases} \quad (7)$$

Thus the freshwater shortage is defined as the freshwater demand that cannot be met, neither by the extraction rate, nor by the freshwater reserves. The $\max\{\cdot\}$ -term in Eq. (7) represents the contribution of whatever is left in the storage to limit the shortage.

In essence, Eq. (7) states that when the demand (D) is larger than the extraction rate (E) — i.e., the supply of freshwater — and what is left of freshwater storage ($\max\{\cdot\}$ -term), shortages occur. These

Table 3

Water intake specifications in the Haringvliet, the Netherlands. V_c : freshwater storage capacity; D freshwater demand; E_{\max} maximum extraction rate. Data provided by the water board Hollandse Delta.

Intake station		V_c [$\times 1000 \text{ m}^3$]	D [m^3s^{-1}]	E_{\max} [m^3s^{-1}]
GK	Gemaal Koert	37	0.70	1.39
GDBP	Gemaal de Bommelse Polders	60	1.33	2.65
IVP	Inlaat van Pallandt	300	4.50	8.96
HBZ	Hevel Beningerwaard Zuidland	75	1.21	2.41
IDH	Inlaat den Hitsert	15	0.36	0.72
GW	Gemaal Westerpolder	12	0.10	0.20

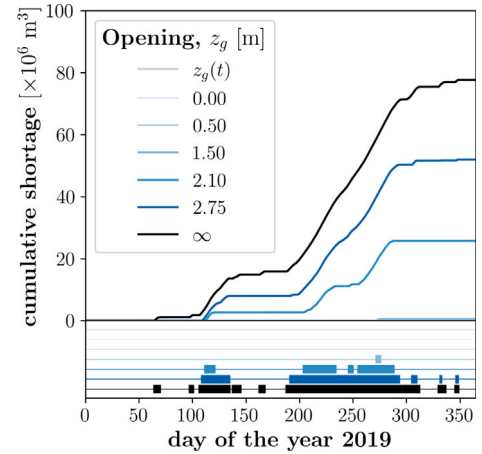


Fig. 2. Freshwater shortages due to opening the Haringvliet sluices. The bars on the bottom display the moments of freshwater shortage, i.e., $S > 0$ (Eq. (7)).

shortages (S) equal the amount of demanded water that cannot be provided by either extracting freshwater, or using available freshwater reserves.

These shortages form the basis of the freshwater performance indicator:

$$P_w = 1 - \frac{\int_T S dt}{\int_T D dt} \in [0, 1] \quad (8)$$

where T is the period of interest [s]; S the freshwater shortage [m^3s^{-1}]; and D the freshwater demand [m^3s^{-1}]. Note that $P_w \in [0, 1]$ follows from the freshwater shortage being bounded by null and the demand, i.e., $0 \leq S \leq D$. In essence, Eq. (8) quantifies how much of the freshwater demand has been met over the period of interest, T .

The Haringvliet and its water intakes are managed under the jurisdiction of Waterschap Hollandse Delta, which covers 100,000s of people — including part of Rotterdam —, substantial agricultural land, and the majority of the Port of Rotterdam. There are six water intakes withdrawing from the Haringvliet and its surroundings, which are listed in Table 3, and their locations are shown in Fig. 1.

3. Results

The impact of opening the Haringvliet sluices on the freshwater availability is non-existent for $z_g \leq 0.50 \text{ m}$ (Fig. 2—including the reference case, $z_g = z_g(t)$). It is for $z_g \geq 1.50 \text{ m}$ that the capacity of the existing water intakes cannot keep up with the demand year-round, although the impact is very limited for $z_g = 1.50 \text{ m}$, which only shows the occurrence of freshwater shortages at the end of the summer.

For $z_g \geq 1.50 \text{ m}$, freshwater shortage increase with increasing the opening (Fig. 2). This relation is strongest between $z_g = 1.50 \text{ m}$ and $z_g = 2.75 \text{ m}$, and becomes less for $z_g > 2.75 \text{ m}$. Thus, there are phases in increased cumulative shortage due to the opening of the gates.

The minor dip in freshwater availability for $z_g = 1.50 \text{ m}$ arises from near-perfect performance ($P_w \geq 0.98$) of the western intakes (Fig. 3(d)),

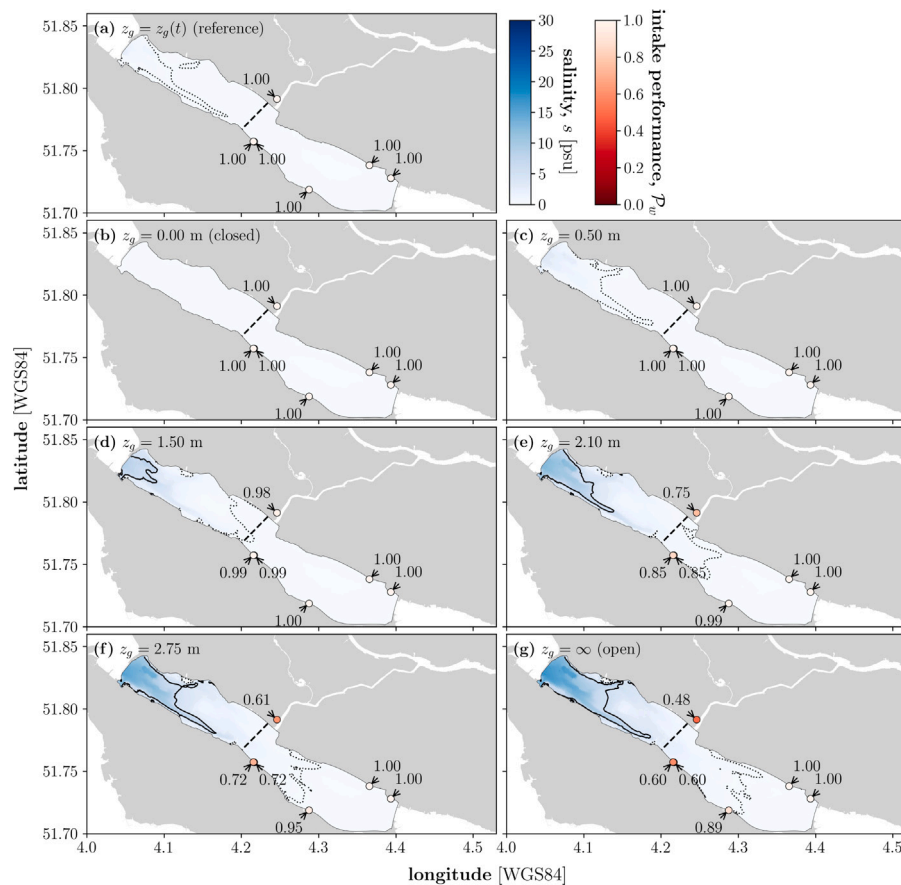


Fig. 3. Annual mean of depth-averaged, tidal salinity maxima and up-time of water intakes. (a) $z_g = z_g(t)$ (reference), (b) $z_g = 0.00$ m (closed), (c) $z_g = 0.50$ m, (d) $z_g = 1.50$ m, (e) $z_g = 2.10$ m, (f) $z_g = 2.75$ m, and (g) $z_g = \infty$ (open). The drinking water salinity threshold of $s_c = 0.27$ psu is marked by the black, dotted contour line; and the freshwater-brackish threshold of $s_s = 5.4$ psu is marked by the black, solid contour line. The black, dashed line indicates the “Middelharnis-Spui line”. (For interpretation of the references to colour in this figure legend, the reader is referred to the web version of this article.)

which are located near the “Middelharnis-Spui line”. Fig. 3 shows that the “Middelharnis-Spui line” is a good indicator of performance loss of the western water intakes, illustrated by the loss of performance as soon as the 0.27-psu isohaline crosses this line. Further opening the gates results in threatening the freshwater availability, eventually also affecting water intakes farther upstream (i.e., GDBP; Fig. 1). The two eastern most water intakes are located outside the zone of impact (i.e., IDH and GW; Fig. 1), even when the gates are completely opened (Fig. 3(g)).

The increasing influence of salinity is also clearly reflected in the ecotope maps (Fig. 4): from a completely freshwater-based ecotope map for a closed Haringvliet ($z_g = 0.00$ m) to an almost completely variable-salinity ecotope map for an open Haringvliet ($z_g = \infty$). However, brackish ecotopes are barely returning to the Haringvliet, despite the salinity reaching levels above the freshwater-brackish threshold of $s_s = 5.4$ psu near the mouth (Fig. 3). This is caused by the variability in salinity that dominates these otherwise brackish regions, which causes the downstream region of the Haringvliet to be mainly classified as variable-salinity (Vx.xx). Note that also large patches of the otherwise freshwater regions are classified as such due to the high variability in salinity.

In addition to the change from freshwater to variable-salinity ecotopes, the hydrodynamic energy in the Haringvliet also increases with increasing opening of the gates as well as increased littoral zones. The increased hydrodynamic activity is concentrated in the channels remnant of the estuary before the closure. Thus, opening the Haringvliet sluices reintroduces the tidal dynamics into the system—or at least partially.

These changes in ecotope area between the various model simulations are clarified in Fig. 5 by means of a Sankey diagram, which contains the system-states as ecotope barcodes: stacked colours whose height represent the relative area occupied by the ecotope with respect to the total area of the area of interest—i.e., the Haringvliet. Such a Sankey diagram shows where ecotopes transition to due to changing conditions, and thus what ecotopes they replace and are replaced by.

As a result of opening the Haringvliet sluices, the Haringvliet transitions from a low-dynamic, freshwater ecosystem to a more diverse system with a highly variable salinity and hydrodynamically active area near the mouth complementary to a low-dynamic, freshwater compartment near the back (Figs. 4 and 5). The level of opening determines the contribution of the variable salinity ecotopes (Fig. 5), and how far these penetrate landward (Fig. 4). Nevertheless, even when the gates are completely opened, a substantial area remains suitable for freshwater ecotopes. Where for $z_g \leq 0.50$ m—including $z_g(t)$ —the Haringvliet is dominated by freshwater, low-energy environments (F2.12), variable salinity, high-energy environments (V2.11) become dominant for $z_g \geq 2.75$ m with substantial contributions of other ecotopes—the sub-littoral dominance remains for all levels of opening. This transition is an expected trend arising from further opening the gates: a transition from freshwater to variable salinity in combination with a transition from low to high energy hydrodynamics.

Opening the Haringvliet sluices clearly affects the freshwater availability negatively, and the ecological diversity positively. This trade-off is presented in Fig. 6 as a Pareto-front: the two performance indicators are plotted against each other to illustrate what the effects are on both perspectives. The further the points in a Pareto-front are from the

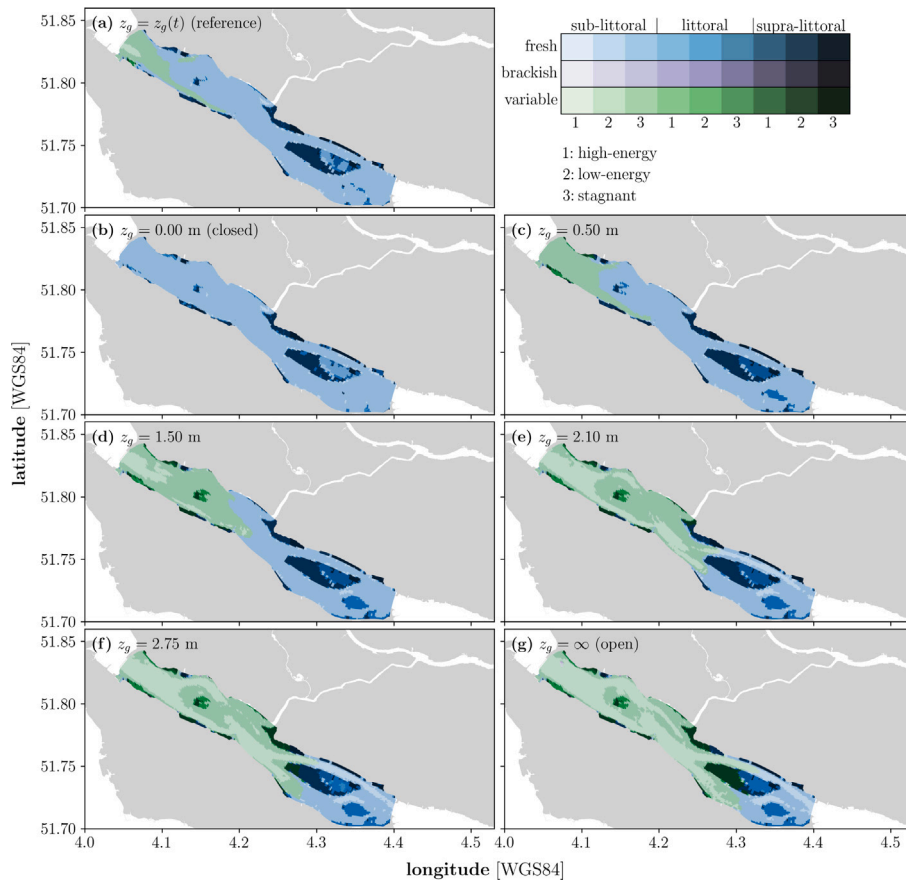


Fig. 4. Ecotope-maps of the Haringvliet. (a) $z_g = z_g(t)$ (reference), (b) $z_g = 0.00$ m (closed), (c) $z_g = 0.50$ m, (d) $z_g = 1.50$ m, (e) $z_g = 2.10$ m, (f) $z_g = 2.75$ m, and (g) $z_g = \infty$ (open). Note that brackish ecotopes appear near the mouth of the Haringvliet with (partially) opened gates, but their contribution is very minimal, i.e., hard to see in the figure.

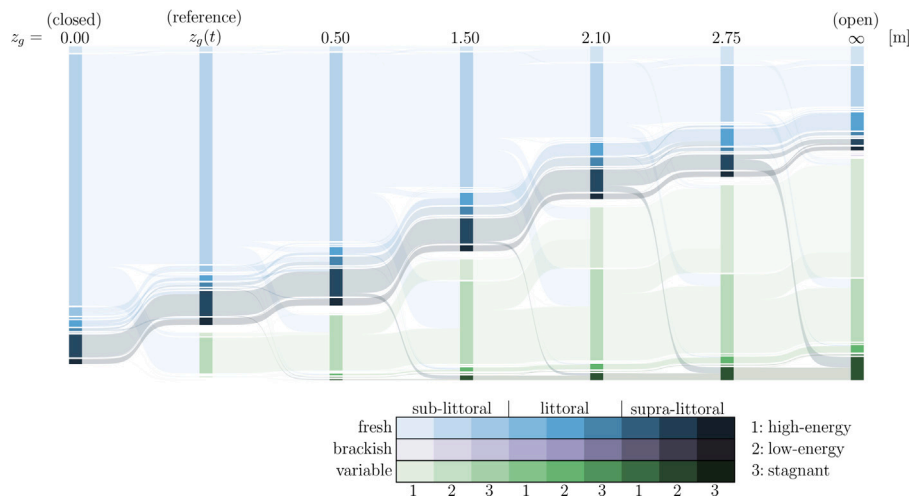


Fig. 5. Sankey diagram of the ecotopes in the Haringvliet. Every ecotope barcode (stacked bar) represents the system’s ecological state by means of the relative areal contribution of every ecotope in the Haringvliet. The ecotope barcodes are connected by how the ecotopes transition between model simulations, i.e., ecological states.

origin, the higher the combined performances; i.e., points closer to the top-right corner in Fig. 6 present more desirable outcomes.

In line with the results presented in Fig. 2, Fig. 6 shows that the freshwater availability remains unaffected up to $z_g = 0.50$ m—and is only barely impacted at $z_g = 1.50$ m. Meanwhile, the ecological performance increases, illustrated by the (almost) vertical line in Fig. 6. Noteworthy is the enhanced ecological diversity in the Haringvliet as

a result of the “Kierbesluit” — i.e., $z_g = z_g(t)$ — without compromising on the freshwater availability (compared to a closed Haringvliet, i.e., $z_g = 0.00$ m). It is not until the western-most water intakes get affected by the increasing salinity in the Haringvliet that the socio-economic performance indicator starts to drop: from a (near) perfect performance for $z_g \leq 1.50$ m to $P_w = 0.70$ for a completely open connection—i.e., $z_g = \infty$.

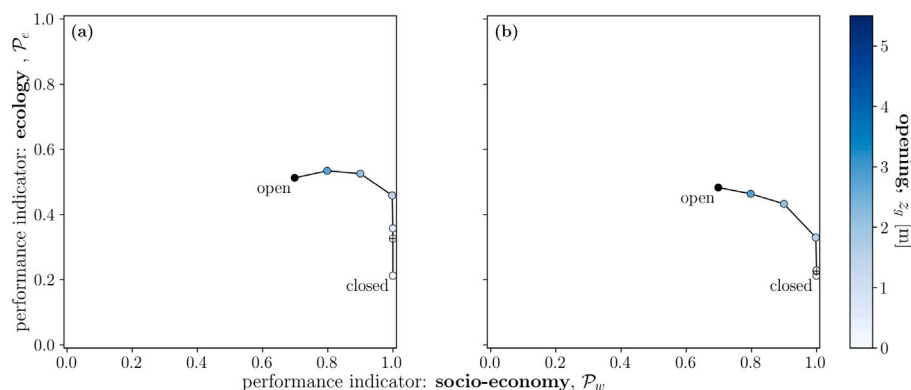


Fig. 6. Pareto-fronts of socio-ecological performance indicators (a) including the variable-salinity class; and (b) excluding the variable-salinity class. The reference case is marked with a plus-sign in the centre; and the completely opened gates are coloured black. (For interpretation of the references to colour in this figure legend, the reader is referred to the web version of this article.)

Interestingly, there is a limit to the added value of the ecological diversity for further opening the gates visible in Fig. 6. At the upper end of the opening heights, the ecotope diversity reduces with increasing opening, reaching an “optimum” at $z_g = 2.75$ m with $P_e = 0.53$ (Fig. 6). Note that this “optimum” is not a real optimum but an artefact following from the definition of the evenness index (Eq. (2)) in combination with the (limited) area of interest: when freshwater ecotopes dominate the Haringvliet, increased opening reduces this dominance causing a more even ecotope distribution. However, when the variable-salinity ecotopes are dominant, further opening the sluices enhances this dominance due to which the evenness index — i.e., the ecological performance indicator (Eq. (2)) — reduces. This change in dominant salinity class is also clearly visible in Figs. 4 and 5. Note that this dip would not be visible if the area of interest would have been extended further upstream.

4. Discussion

The Haringvliet sluices and their opening regime have a significant effect on the ecotope diversity as well as the freshwater availability. However, opening the gates only slightly — i.e., $z_g \leq 0.50$ m — improves the diversity without compromising on the freshwater availability (Fig. 6). Thus aside from re-establishing the connectivity between the Haringvliet and the North Sea for fish migration (Baas et al., 2020; Bice et al., 2023), the “Kierbesluit” also supports the development of a more diverse set of ecotopes in the Haringvliet (Fig. 4(a) and (b)).

In addition to the increased saline influence in the Haringvliet due to opening the gates, this opening also reintroduces the tidal fluctuations in the system. The (partial) removal of the tidal breathing in an estuary is a common side-effect of large-scale interventions such as storm surge barriers (e.g., Ralston, 2022; Nienhuis and Smaal, 1994). However, the ecological benefits and water quality improvements achieved by reintroducing tidal dynamics are often stressed by nature restoration projects (e.g., Abbott et al., 2020; Glamore et al., 2021; Heimhuber et al., 2024). The intertidal areas arising from tidal dynamics are ecologically valuable, providing several crucial ecosystem services (e.g., Barbier et al., 2011; Costanza et al., 1997), and have been found to reduce methane emissions of wetlands (Kroeger et al., 2017; Rosentreter et al., 2021).

For (partial) reintroduction of the tidal dynamics in the Haringvliet, the gates need to be opened to $z_g \geq 1.50$ m, which would more than double the littoral zone compared to a closed system (from 3.4% to 9.8% of the area; Fig. 7), while the supra-littoral zone remains similar (around 9%–12%). Thus partially opening the gates would restore the dynamics in the Haringvliet, comparable to fully opening the gates. Note that even when the Haringvliet sluices are completely closed,

there is still some intertidal area (Fig. 7(b)) — i.e., tidal dynamics — due to its connectivity to the North Sea via the many branches of the Rhine-Meuse Delta. The “Kierbesluit” opening regime does little to enhance the littoral zone in the Haringvliet, while a permanent opening of $z_g = 0.50$ m — which is comparable to the time-averaged opening of the “Kierbesluit” — would almost double the littoral zone.

The aforementioned ecological value of intertidal areas can also be used as a (restoration) goal with the implemented assessment method: The ecotope barcodes (i.e., Fig. 5) allow us to focus on specific, desired ecotopes that are considered (very) valuable and ecologically desirable. An example of such a focused assessment is presented in Fig. 8 in which we highlight the presence of intertidal areas (i.e., xx.2x). The presence of this valuable collection of ecotopes clearly increases with increasing opening of the Haringvliet sluices (Fig. 8), with the steepest increase for $z_g \leq 1.50$ m.

Note, however, that the rare brackish, estuarine ecosystem present in the Haringvliet before its closure (Tangelder et al., 2017) remains virtually absent, even with the gates completely opened (Fig. 4(g)). Although salinity levels are sufficiently high near the Haringvliet sluices to support a brackish ecosystem (Fig. 3(e)–(g)), the variability in salinity is such that this area is classified as variable-salinity (i.e., Vx.xx). This is related to the dominance and variability in freshwater input from the rivers. As a result, regions in the Haringvliet can become completely fresh and exceed well beyond the marine salinity threshold of 18 psu within a single year.

In addition, when fully opening the gates, there remain two major differences compared to pre-closure: (1) part of the mouth of the Haringvliet is dammed off, which blocks the river outflow even when the gates are fully opened (Fig. 1); and (2) the Grevelingen — the waterbody south of the Haringvliet — has been closed since pre-closure times, which causes a concentration of river outflow through the Haringvliet. Due to the above two differences, more fresh river water is pushed through the Haringvliet, which likely makes its waters fresher than before its closure; hence, the large variability in salinity in the Haringvliet.

However, the use of the variable-salinity classification — as proposed by Bouma et al. (2005) and adopted in this study — is not common; e.g., in their reflection on the loss of rare brackish, estuarine ecosystems, Tangelder et al. (2017) do not consider variable-salinity as a class on the salinity-scale. Furthermore, the minimum in species-richness in the classic model of Remane (1934) for brackish systems is attributed to the variability in salinity. This would question the use of a variable-salinity class. Whether the variable-salinity classification can be discarded is open for debate, as the salinity variance has been found to have a significant impact on brackish ecosystems (Van Diggelen and Montagna, 2016). If we would discard the variable-salinity classification, we can see in Fig. 3(d)–(g) that brackish conditions return in the

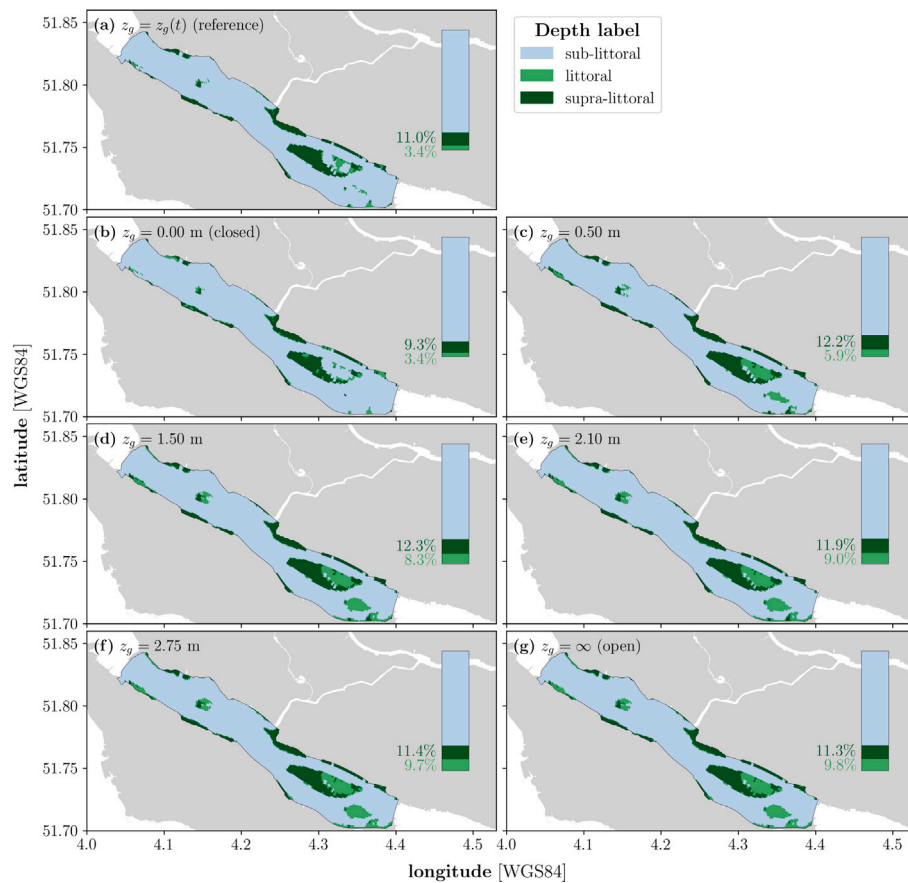


Fig. 7. Littoral zoning in the Haringvliet. (a) $z_g = z_g(t)$ (reference), (b) $z_g = 0.00$ m (closed), (c) $z_g = 0.50$ m, (d) $z_g = 1.50$ m, (e) $z_g = 2.10$ m, (f) $z_g = 2.75$ m, and (g) $z_g = \infty$ (open). The bar-charts in the upper-right corners present the areal percentage of the intertidal area in the Haringvliet. Intertidal areas represent the littoral zone, which ranges between mean-low-water-spring (MLWS) and mean-high-water-neap (MHWN) according to EMMA (Bouma et al., 2005; Brunink and Hendrickx, 2024).

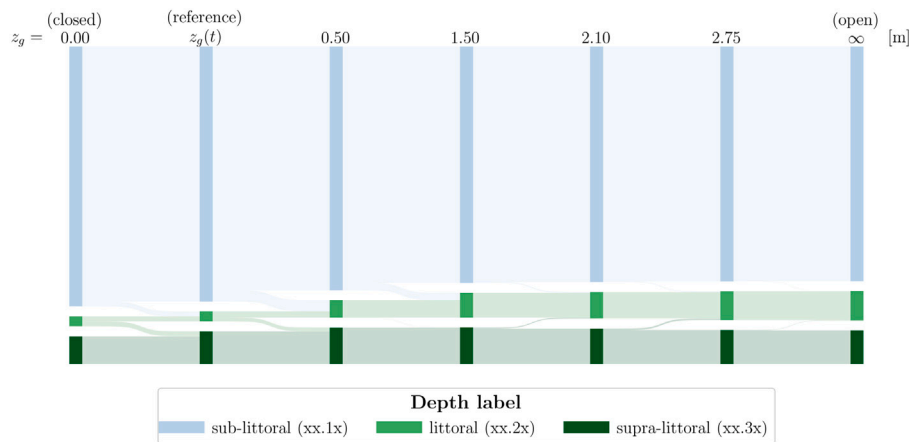


Fig. 8. Sankey-diagram focused on littoral zoning. Every ecotope barcode represents the relative areal contribution to the Haringvliet.

Haringvliet for $z_g \geq 1.50$ m, which would indicate a restoration of the rare brackish, estuarine ecosystems in the Haringvliet when the gates are (partially) opened.

For the determination of the ecotopes, we simulated the year 2019, which was a representative year regarding river discharges: A Z-score of -0.57 over the last 120 years, and a Z-score of -0.59 over the last 30 years (Geraeds et al., in review). Such long-term representative conditions are preferred for the use of EMMA (Bouma et al., 2005; Brunink and Hendrickx, 2024). However, the functioning of the freshwater intakes is most stressed during droughts and storms, when

there is limited freshwater inflow into the Haringvliet to mitigate salt intrusion. Therefore, the impact of (partially) opening the gates is expected to be more detrimental during droughts and storms than the results shown in this study (Fig. 2), likely hampering the freshwater performance—i.e., moving the front in Fig. 6 leftward.

During such dry and stormy periods, a crisis policy of closing the gates temporarily to secure the freshwater availability could be adopted. Such a crisis policy would fit in nicely in adaptive management strategies. Note, however, that a closed Haringvliet is not completely safe from saline influences, as saline water can still enter

via the Spui — the northern branch connected to the North Sea (Fig. 1) —, causing saline contamination (Gerritsma et al., 2025). An additional measure could include a larger capacity of the eastern water intakes, i.e., increase their maximum extraction capacity and/or their storage capacity. Such an enlarged capacity of the eastern water intakes would also allow for opening the gates to $z_g \geq 1.50$ m during “normal” conditions.

As the model simulations are expensive to execute, a multi-year analysis would be computationally (too) demanding. Instead, a scenario-based analysis could be used to gain insights into the socio-ecological trade-off under differing conditions. Where this study has presented such an analysis for “normal” conditions, follow-up studies could expand on our work by analysing dry and/or storm conditions, and how they change the socio-ecological trade-off presented in this study (e.g., Fig. 6).

Although inherently incomplete, the performance indicators as defined in this study are illustrative of the socio-ecological trade-off associated with the opening regime of the Haringvliet sluices. The resulting Pareto-front as presented in Fig. 6 is an intuitive visualization of the trade-off between — in our case — socio-ecological interests. The overall performance of the collection of performance indicators can be determined by the square area under the curve (e.g., Emmerich and Deutz, 2018), i.e., the square consisting of the origin and (P_w, P_e) . Therefore, the Pareto-front is a useful tool for decision- and policy-makers, and aids in communicating the trade-offs between different measures to the general public.

Note that the performance indicators as presented in Fig. 6 purposefully exclude any valuation, which is a subjective and political matter affected by the zeitgeist. However, this is a key-step in decision- and policy-making, and can be achieved by the definition of valuation functions (Greco et al., 2016; Keeney and Raiffa, 1993, for approaches to define such valuation functions). These valuation functions can be embedded in the intuitive visualization of Pareto-fronts, maintaining their benefits in decision- and policy-making as well as communication to the public (Bakker et al., 2025, for the embedding of valuation functions).

The use of Pareto-fronts requires the quantification of performance indicators, which is where the contribution of EMMA to explore the potential ecological impact of different interventions is crucial. In addition to the subsequently derived diversity- and evenness-indices (Eqs. (1) and (2)), the ecotope barcodes allow us to focus on specific, desired ecotopes, and provide the basis for translating ecotopes to location-specific indicators such as ecosystem services. Goals could be set to ensure a minimum area for a specific ecotope — or set of ecotopes — that is considered of great ecological value, e.g., intertidal areas (Fig. 8). This method allows ecological interests to be set on equal footing with other stakeholders’ interests, and a quantification of the ecological costs and benefits of large-scale, estuarine interventions.

5. Conclusion

In this study, we have implemented a hydrodynamic model to explore the effects of reopening the Haringvliet sluices on a socio-ecological trade-off: freshwater availability versus ecological diversity. The presented socio-ecological evaluation has shown that the ecological potential of the Haringvliet could substantially increase by opening the Haringvliet sluices—at least partially. The impact on the freshwater availability is expected to be limited up to an opening of $z_g = 1.50$ m. However, we did so for a representative year regarding river discharges and storm surges — required for the ecological assessment —, while freshwater availability is more seriously threatened during drought and storm conditions.

The use of representative (non-monetary) performance indicators for the considered stakeholders allowed us to demonstrate the trade-offs in a clear fashion: the Pareto-front resulting from these performance indicators is an intuitive visualization of the costs and benefits between

stakeholders. In particular, the use of EMMA allowed us to explore and quantify the ecological implications of estuary-scale interventions, such as (partially) opening the Haringvliet sluices. We have thereby presented an approach in which ecological interests can be set on equal footing with other stakeholders’ interests allowing for a similar incorporation of ecological implications in decision- and policy-making.

CRediT authorship contribution statement

Gijs G. Hendrickx: Writing – review & editing, Writing – original draft, Visualization, Methodology, Investigation, Formal analysis, Conceptualization. **Gregory S. Fivash:** Writing – review & editing, Methodology, Conceptualization. **Avelon Gerritsma:** Writing – review & editing, Data curation. **Marlein Geraeds:** Writing – review & editing, Data curation. **Stuart G. Pearson:** Writing – review & editing, Supervision, Conceptualization.

Software availability

This study builds upon the open-access tool EMMA (Ecotope-Map Maker based on Abiotics; Hendrickx and Brunink, 2023), which is a Python-based processing tool translating hydrodynamic model output data to ecotope potential maps.

Funding

This publication is part of the project “Design and operation of nature-based SALTISolutions” (with project number P18-32 Project 7) of the research programme SALTISolutions which is (partly) financed by the Dutch Research Council (NWO). SP is funded by project 21026 Revealing Hidden Networks of Coastal Sediment Pathways via Laboratory & Numerical Experiments, supported by the Dutch Research Council (NWO).

Declaration of competing interest

The authors declare the following financial interests/personal relationships which may be considered as potential competing interests: Gijs G. Hendrickx reports financial support was provided by Nederlandse Organisatie voor Wetenschappelijk Onderzoek (NWO). Stuart G. Pearson reports financial support was provided by Nederlandse Organisatie voor Wetenschappelijk Onderzoek (NWO). Gijs G. Hendrickx reports equipment, drugs, or supplies was provided by SURF Cooperative. If there are other authors, they declare that they have no known competing financial interests or personal relationships that could have appeared to influence the work reported in this paper.

Acknowledgements

We are indebted to Peter M.J. Herman for his contributions to the early stages of the research design, which greatly added value to the study and subsequent manuscript. We would also like to thank Thijs IJpelaar and Jermo de Miranda (Hoogheemraadschaap Hollandse Delta) for providing information about the water intakes included in this study. This work used the Dutch national e-infrastructure with the support of the SURF Cooperative using grant no. EINF-7152. At last, we would also like to thank the four anonymous reviewers for their valuable feedback on the original manuscript; their suggestions greatly improved the paper.

Data availability

Data will be made available on request.

References

- Abbott, B., Wallace, J., Nicholas, D., Karim, F., Waltham, N., 2020. Bund removal to re-establish tidal flow, remove aquatic weeds and restore coastal wetland services—North queensland, Australia. *PLoS One* 15 (1), e0217531. <http://dx.doi.org/10.1371/journal.pone.0217531>, <https://dx.plos.org/10.1371/journal.pone.0217531>.
- Baas, V., Clabbers, N., Moens, J., Schuurke, E., Spierings, J., Termaat, E., Wolma, A., 2020. Opening of the Haringvliet: A Stream of Possibilities. Tech. Rep., Wageningen University, Wageningen, the Netherlands.
- Bakker, F., Hendrickx, G., Keyzer, L., Iglesias, S., Aarninkhof, S., van Koningsveld, M., 2025. Trading off dissimilar stakeholder interests: Changing the bed level of the main shipping channel of the rhine-Meuse Delta while considering freshwater availability. *Environ. Challenges* 21, 101323. <http://dx.doi.org/10.1016/j.envc.2025.101323>.
- Barbier, E., Hacker, S., Kennedy, C., Koch, E., Stier, A., Silliman, B., 2011. The value of estuarine and coastal ecosystem services. *Ecol. Monograph* 81 (2), 169–193. <http://dx.doi.org/10.1890/10-1510.1>.
- Beeldman, P., Workel, K., de Rooy, M., 2018. Re-opening the rhine river for fish. In: Brink, K., Gough, P., Royte, J., Schollema, P., Wannings, H. (Eds.), *From Sea To Source 2.0: Protection and Restoration of Fish Migration in Rivers Worldwide*. World Fish Migration Foundation, Groningen, the Netherlands, pp. 234–241.
- Bice, C., Huisman, J., Kimball, M., Mallen-Cooper, M., Zampatti, B., Gillanders, B., 2023. Tidal barriers and fish – impacts and remediation in the face of increasing demand for freshwater and climate change. *Estuar. Coast. Shelf Sci.* 289, 108376. <http://dx.doi.org/10.1016/j.ecss.2023.108376>, <https://linkinghub.elsevier.com/retrieve/pii/S0272771423000166X>.
- Bol, R., Kraak, A., 1998. Water- en zoutbeweging. In: van Hees, J., Peters, H. (Eds.), *MER beheer Haringvlietstuiven: Over de grens van zoet en zout*. Rotterdam, p. 211.
- Bouma, H., de Jong, D., Twisk, F., Wolfstein, K., 2005. A Dutch Ecotope System for Coastal Waters (ZES.1). Tech. Rep., Rijkswaterstaat, Rijksinstituut voor Kust en Zee, Middelburg, the Netherlands.
- Breine, J., Maes, J., Ollevier, F., Stevens, M., 2011. Fish assemblages across a salinity gradient in the zeeschelde estuary (Belgium). *Belgian J. Zool.* 141 (2), 21–44.
- Brevé, N., Vis, H., Breukelaar, A., 2019. Escape from the north sea: the possibilities for pikeperch (*sander lucioperca* l. 1758) to re-enter the rhine and meuse estuary via the haringvlietdam, as revealed by telemetry. *J. Coast. Conserv.* 23 (1), 239–252. <http://dx.doi.org/10.1007/s11852-018-0654-5>, <https://link.springer.com/article/10.1007/s11852-018-0654-5> <http://link.springer.com/10.1007/s11852-018-0654-5>.
- Brunink, S., Hendrickx, G., 2024. Predicting ecotopes from hydrodynamic model data: Towards an ecological assessment of nature-based solutions. *Nature-Based Solutions* 6, 100145. <http://dx.doi.org/10.1016/j.nbsj.2024.100145>, <https://linkinghub.elsevier.com/retrieve/pii/S2772411524000363>.
- Cloern, J., Jassby, A., Schraga, T., Nejad, E., Martin, C., 2017. Ecosystem variability along the estuarine salinity gradient: Examples from long-term study of san francisco bay. *Limnol. Oceanogr.* 62 (S1), S272–S291. <http://dx.doi.org/10.1002/lno.10537>, <https://aslopubs.onlinelibrary.wiley.com/doi/10.1002/lno.10537>.
- Costa, Y., Martins, I., de Carvalho, G., Barros, F., 2023. Trends of sea-level rise effects on estuaries and estimates of future saline intrusion. *Ocean. Coast. Manag.* 236, 106490. <http://dx.doi.org/10.1016/j.ocecoaman.2023.106490>.
- Costanza, R., D'Arge, R., de Groot, R., Farber, S., Grasso, M., Hannon, B., et al., 1997. The value of the world's ecosystem services and natural capital. *Nature* 387 (6630), 253–260. <http://dx.doi.org/10.1038/387253a0>, <https://www.nature.com/articles/387253a0>.
- de Vriend, H., Wang, Z., Ysebaert, T., Herman, P., Ding, P., 2011. Eco-morphological problems in the Yangtze Estuary and the western scheldt. *Wetlands* 31 (6), 1033–1042. <http://dx.doi.org/10.1007/s13157-011-0239-7>, <https://link.springer.com/10.1007/s13157-011-0239-7>.
- van Dijk, W., Cox, J., Leuven, J., Cleveringa, J., Taal, M., Hiatt, M., et al., 2021. The vulnerability of tidal flats and multi-channel estuaries to dredging and disposal. *Anthr. Coasts* 4 (1), 36–60. <http://dx.doi.org/10.1139/anc-2020-0006>, <https://link.springer.com/10.1139/anc-2020-0006>.
- Elmqvist, T., Folke, C., Nyström, M., Peterson, G., Bengtsson, J., Walker, B., Norberg, J., 2003. Response diversity, ecosystem change, and resilience. *Front. Ecol. Environ.* 1 (9), 488–494. [http://dx.doi.org/10.1890/1540-9295\(2003\)001\[0488:RDECAR\]2.0.CO;2](http://dx.doi.org/10.1890/1540-9295(2003)001[0488:RDECAR]2.0.CO;2).
- Emmerich, M., Deutz, A., 2018. A tutorial on multiobjective optimization: Fundamentals and evolutionary methods. *Nat. Comput.* 17 (3), 585–609. <http://dx.doi.org/10.1007/s11047-018-9685-y>, <https://link.springer.com/article/10.1007/s11047-018-9685-y> <http://link.springer.com/10.1007/s11047-018-9685-y>.
- Fairchild, T., Bennett, W., Smith, G., Day, B., Skov, M., Möller, I., ...Griffin, J., 2021. Coastal wetlands mitigate storm flooding and associated costs in estuaries. *Environ. Res. Lett.* 16 (7), 074034. <http://dx.doi.org/10.1088/1748-9326/ac0c45>, <https://iopscience.iop.org/article/10.1088/1748-9326/ac0c45> <https://iopscience.iop.org/article/10.1088/1748-9326/ac0c45/meta>.
- Figueroa, S., Lee, G., Chang, J., Jung, N., 2022. Impact of estuarine dams on the estuarine parameter space and sediment flux decomposition: Idealized numerical modeling study. *J. Geophys. Res.: Ocean.* 127, <http://dx.doi.org/10.1029/2021JC017829>, e2021JC017829, <https://agupubs.onlinelibrary.wiley.com/doi/10.1029/2021JC017829>.
- Folke, C., Carpenter, S., Elmqvist, T., Gunderson, L., Holling, C., Walker, B., 2002. Resilience and sustainable development: Building adaptive capacity in a world of transformations. *AMBIO: A J. Hum. Environ.* 31 (5), 437–440. <http://dx.doi.org/10.1579/0044-7447-31.5.437>, <http://www.bioone.org/doi/abs/10.1579/0044-7447-31.5.437>.
- Galván, C., Puente, A., Juanes, J., 2021. Nested socio-ecological maps as a spatial planning instrument for estuary conservation and ecosystem-based management. *Front. Mar. Sci.* 8, <http://dx.doi.org/10.3389/fmars.2021.730762>.
- Geraeds, M., Pietrzak, J., Gerritsma, A., Verlaan, M., Katsman, C., in review. Assessing the importance of the near-field plume state on estuarine dynamics under varying wind directions. *J. Geophys. Res.: Ocean.* <https://doi.org/10.22541/essoar.174534309.94419306.v1>.
- Gerritsma, A., Verlaan, M., Geraeds, M., Huismans, Y., Pietrzak, J., 2025. The effects of a storm surge event on salt intrusion: Insights from the Rhine-Meuse Delta. *J. Geophys. Res.: Ocean.* 130 (4), <http://dx.doi.org/10.1029/2024JC021520>, e2024JC021520.
- Glamore, W., Rayner, D., Ruprecht, J., Sadat-Noori, M., Khojasteh, D., 2021. Ecohydrology as a driver for tidal restoration: Observations from a Ramsar wetland in eastern Australia. *PLoS One* 16 (8), e0254701. <http://dx.doi.org/10.1371/journal.pone.0254701>.
- Granek, E., Polasky, S., Kappel, C., Reed, D., Stoms, D., Koch, E., Wolanski, E., 2010. Ecosystem services as a common language for coastal ecosystem-based management. *Conserv. Biol.* 24 (1), 207–216. <http://dx.doi.org/10.1111/j.1523-1739.2009.01355.x>, <https://conbio.onlinelibrary.wiley.com/doi/10.1111/j.1523-1739.2009.01355.x>.
- Greco, S., Figueira, J., Ehgott, M., 2016. *Multiple Criteria Decision Analysis: State of the Art Surveys*, second ed. Springer.
- de la Haye, M., Reeze, B., van der Jagt, H., Verweij, G., 2022. Vervolgrapportage ecologische toestand Haringvliet en Voordelta 'Lerend implementeren kierbesluit' 2020. Tech. Rep., Bureau Waardenburg, Culemborg, the Netherlands.
- Heimhuber, V., Raoult, V., Glamore, W., Taylor, M., Gaston, T., 2024. Restoring blue carbon ecosystems unlocks fisheries' potential. *Restoration Ecol.* 32 (1), e14052. <http://dx.doi.org/10.1111/rec.14052>, <https://onlinelibrary.wiley.com/doi/10.1111/rec.14052>.
- Hendrickx, G., Brunink, S., 2023. EMMA: Ecotope-Map Maker based on Abiotics. 4TU.ResearchData, <http://dx.doi.org/10.4121/0100fc5a-a99c-4002-9864-3faade3899e3.v1>.
- Hooper, D., Chapin, F., Ewel, J., Hector, A., Inchausti, P., Lavorel, S., et al., 2005. Effects of biodiversity on ecosystem functioning: A consensus of current knowledge. *Ecol. Monograph* 75 (1), 3–35. <http://dx.doi.org/10.1890/04-0922>, <https://esajournals.onlinelibrary.wiley.com/doi/10.1890/04-0922> <http://doi.wiley.com/10.1890/04-0922>.
- Hop, J., Vriese, F., 2011. *Vismigratie Rijn-Maasstroomgebied*. Tech. Rep., ATKb, Rotterdam, the Netherlands.
- Jones, E., Bierkens, M., Wanders, N., Sutanudjaja, E., van Beek, L., van Vliet, M., 2023. DynQual v1.0: a high-resolution global surface water quality model. *Geosci. Model. Dev.* 16 (15), 4481–4500. <http://dx.doi.org/10.5194/gmd-16-4481-2023>, <https://gmd.copernicus.org/articles/16/4481/2023/>.
- Keeney, R., Raiffa, H., 1993. *Decisions with Multiple Objectives*. Cambridge University Press, Cambridge, United Kingdom, <http://dx.doi.org/10.1017/cbo9781139174084>, <https://www.cambridge.org/core/books/decisions-with-multiple-objectives/DEF338459C32778C3F8C4C4A682032F> <https://www.cambridge.org/core/product/identifier/9781139174084/type/book>.
- Kernkamp, H., Van Dam, A., Stelling, G., de Goede, E., 2011. Efficient scheme for the shallow water equations on unstructured grids with application to the continental shelf. *Ocean. Dyn.* 61 (8), 1175–1188. <http://dx.doi.org/10.1007/s10236-011-0423-6>, <http://link.springer.com/10.1007/s10236-011-0423-6>.
- Kranenburg, W., Tiessen, M., Blaas, M., Van Veen, N., 2023. Circulation, stratification and salt dispersion in a former estuary after reintroducing seawater inflow. *Estuar. Coast. Shelf Sci.* 282, 108221. <http://dx.doi.org/10.1016/j.ecss.2023.108221>, <https://linkinghub.elsevier.com/retrieve/pii/S0272771423000112>.
- Kroeger, K., Crooks, S., Moseman-Valtierra, S., Tang, J., 2017. Restoring tides to reduce methane emissions in impounded wetlands: A new and potent blue carbon climate change intervention. *Sci. Rep.* 7 (1), 11914. <http://dx.doi.org/10.1038/s41598-017-12138-4>, <https://www.nature.com/articles/s41598-017-12138-4>.
- Kubicek, A., Breckling, B., Hoegh-Guldberg, O., Reuter, H., 2019. Climate change drives trait-shifts in coral reef communities. *Sci. Rep.* 9 (1), 3721. <http://dx.doi.org/10.1038/s41598-019-38962-4>, <http://www.nature.com/articles/s41598-019-38962-4>.
- Limberger, R., Daugaard, U., Gupta, A., Krug, R., Lemmen, K., van Moorsel, S., Petchey, O., 2023. Functional diversity can facilitate the collapse of an undesirable ecosystem state. *Ecol. Lett.* 26 (6), 883–895. <http://dx.doi.org/10.1111/ele.14217>, <https://onlinelibrary.wiley.com/doi/10.1111/ele.14217>.
- Liquete, C., Piroddi, C., Drakou, E., Gurney, L., Katsanevakis, S., Charef, A., Egoh, B., 2013. Current status and future prospects for the assessment of marine and coastal ecosystem services: A systematic review. *PLoS One* 8 (7), e67737. <http://dx.doi.org/10.1371/journal.pone.0067737>.
- Loreau, M., Mouquet, N., Gonzalez, A., 2003. Biodiversity as spatial insurance in heterogeneous landscapes. *Proc. Natl. Acad. Sci. USA* 100 (22), 12765–12770. <http://dx.doi.org/10.1073/pnas.2235465100>, <https://www.pnas.org/doi/abs/10.1073/pnas.2235465100> <https://pnas.org/doi/full/10.1073/pnas.2235465100>.

- Loreau, M., Naeem, S., Inchausti, P., Bengtsson, J., Grime, J., Hector, A., Wardle, D., 2001. Biodiversity and ecosystem functioning: Current knowledge and future challenges. *Science* 294 (5543), 804–808. <http://dx.doi.org/10.1126/science.1064088>, <https://www.science.org/doi/10.1126/science.1064088>.
- Maul, G., Duedall, I., 2019. Demography of coastal populations. *Encyclopedia of Coastal Science*. Springer International Publishing, pp. 692–700. http://dx.doi.org/10.1007/978-3-319-93806-6_115,
- Medeiros, J., Chaves, M., Silva, G., Azeda, C., Costa, J., Marques, J., et al., 2012. Benthic condition in low salinity areas of the mira estuary (Portugal): Lessons learnt from freshwater and marine assessment tools. *Ecol. Indic.* 19, 79–88. <http://dx.doi.org/10.1016/j.ecolind.2011.09.008>.
- Mestdagh, S., Fang, X., Soetaert, K., Ysebaert, T., Moens, T., Van Colen, C., 2020. Seasonal variability in ecosystem functioning across estuarine gradients: The role of sediment communities and ecosystem processes. *Mar. Environ. Res.* 162, 105096. <http://dx.doi.org/10.1016/j.marenvres.2020.105096>, <https://linkinghub.elsevier.com/retrieve/pii/S0141113620300787>.
- del Moral, R., Fleming, R., 1980. Structure of coniferous forest communities in western washington: Diversity and ecotone properties. *Vegetatio* 41 (3), 143–153. <http://dx.doi.org/10.1007/BF00052443>.
- Muller, J., 2021. The perils of metric fixation. *Med. Teach.* 43 (6), 622–624. <http://dx.doi.org/10.1080/0142159X.2020.1840745>.
- Muller, J., Chen, Y.-p., Aarminkhof, S., Chan, Y.-C., Piersma, T., van Maren, D., et al., 2020. Ecological impact of land reclamation on jiangsu coast (China): A novel ecotone assessment for tongzhou bay. *Water Sci. Eng.* 13 (1), 57–64. <http://dx.doi.org/10.1016/j.wse.2020.04.001>.
- Mzezewa, J., Misi, T., van Rensburg, L., 2010. Characterisation of rainfall at a semi-arid ecotone in the limpopo province (South Africa) and its implications for sustainable crop production. *Water SA* 36 (1), 19–26. <http://dx.doi.org/10.4314/WSA.V36I1.50903>.
- Neumann, B., Vafeidis, A., Zimmermann, J., Nicholls, R., 2015. Future Coastal population growth and exposure to sea-level rise and coastal flooding - a global assessment. *PLOS ONE* 10 (3), e0118571. <http://dx.doi.org/10.1371/journal.pone.0118571>, <https://dx.plos.org/10.1371/journal.pone.0118571>.
- Nienhuis, P., Smaal, A., 1994. The oosterschelde estuary, a case-study of a changing ecosystem: an introduction. *Hydrobiologia* 282–283 (1), 1–14. <http://dx.doi.org/10.1007/BF00024616>, <https://linkinghub.elsevier.com/retrieve/pii/0022098195900705> <http://link.springer.com/10.1007/BF00024616>.
- Orton, P., Ralston, D., van Prooijen, B., Secor, D., Ganju, N., Chen, Z., Marcell, K., 2023. Increased utilization of storm surge barriers: A research agenda on estuary impacts. *Earth's Futur.* 11, <http://dx.doi.org/10.1029/2022EF002991>, e2022EF002991. <https://agupubs.onlinelibrary.wiley.com/doi/10.1029/2022EF002991>.
- Paree, E., 2021. Toelichting op de zoute ecotopenkaart Westerschelde 2020: Biologische monitoring zoute rijkswateren. Tech. Rep., Rijkswaterstaat, Rotterdam, the Netherlands, https://puc.overheid.nl/rijkswaterstaat/doc/PUC_642216_31/1/.
- Pielou, E., 1966. The measurement of diversity in different types of biological collections. *J. Theoret. Biol.* 13 (C), 131–144. [http://dx.doi.org/10.1016/0022-5193\(66\)90013-0](http://dx.doi.org/10.1016/0022-5193(66)90013-0), <https://linkinghub.elsevier.com/retrieve/pii/0022519366900130>.
- Radoux, J., Bourdouxhe, A., Coos, W., Dufrière, M., Defourny, P., 2019. Improving ecotone segmentation by combining topographic and spectral data. *Remote. Sens.* 11 (3), <http://dx.doi.org/10.3390/RS11030354>.
- Ralston, D., 2022. Impacts of storm surge barriers on drag, mixing, and exchange flow in a partially mixed estuary. *J. Geophys. Res.: Ocean.* 127 (4), 1–21. <http://dx.doi.org/10.1029/2021JC018246>.
- Remane, A., 1934. Die brackwasserfauna. *Verhandlungen der Dtsch. Zool. Ges.* 36, 34–74, <https://www.vliz.be/imisdocs/publications/ocrd/214770.pdf>.
- Rosentreter, J., Borges, A., Deemer, B., Holgerson, M., Liu, S., Song, C., et al., 2021. Half of global methane emissions come from highly variable aquatic ecosystem sources. *Nat. Geosci.* 14 (4), 225–230. <http://dx.doi.org/10.1038/s41561-021-00715-2>, <https://www.nature.com/articles/s41561-021-00715-2>.
- Shannon, C., 1948. A mathematical theory of communication. *Bell Syst. Tech. J.* 27 (4), 623–656. <http://dx.doi.org/10.1002/j.1538-7305.1948.tb00917.x>.
- Smaal, A., Nienhuis, P., 1992. The eastern scheldt (the netherlands), from an estuary to a tidal bay: A review of responses at the ecosystem level. *Neth. J. Sea Res.* 30 (C), 161–173. [http://dx.doi.org/10.1016/0077-7579\(92\)90055-J](http://dx.doi.org/10.1016/0077-7579(92)90055-J), <https://linkinghub.elsevier.com/retrieve/pii/007775799290055J>.
- Smith, J., Free, C., Lopazanski, C., Brun, J., Anderson, C., Carr, M., et al., 2023. A marine protected area network does not confer community structure resilience to a marine heatwave across coastal ecosystems. *Global Change Biol.* 29 (19), 5634–5651. <http://dx.doi.org/10.1111/gcb.16862>, <https://onlinelibrary.wiley.com/doi/10.1111/gcb.16862>.
- Stelling, G., van Kester, J., 1994. On the approximation of horizontal gradients in sigma co-ordinates for bathymetry with steep bottom slopes. *Internat. J. Numer. Methods Fluids* 18 (10), 915–935. <http://dx.doi.org/10.1002/fld.1650181003>, <https://onlinelibrary.wiley.com/doi/10.1002/fld.1650181003>.
- Tangelder, M., Winter, E., Ysebaert, T., 2017. Ecologie Van Zoet-Zout Overgang in Deltagebieden: Literatuurstudie En Beoordeling Van Een Scenario in Het Volkerak-Zoommeer. Tech. Rep., Wageningen University & Research, Wageningen, the Netherlands, <http://dx.doi.org/10.18174/436428>, <https://research.wur.nl/en/publications/b2533e9f-2355-48e0-99d5-d1efaf95ecb9>.
- Temmerman, S., Meire, P., Bouma, T., Herman, P., Ysebaert, T., de Vriend, H., 2013. Ecosystem-based coastal defence in the face of global change. *Nature* 504 (7478), 79–83. <http://dx.doi.org/10.1038/nature12859>, <https://www.nature.com/articles/nature12859>.
- Timmerman, A., Haasnoot, M., Middelkoop, H., Bouma, T., McEvoy, S., 2021. Ecological consequences of sea level rise and flood protection strategies in shallow coastal systems: A quick-scan barcoding approach. *Ocean Coasts Management* 210, 105674. <http://dx.doi.org/10.1016/j.ocecoaman.2021.105674>, <https://linkinghub.elsevier.com/retrieve/pii/S0964569121001587>.
- Tönis, I., Stam, J., van de Graaf, J., 2002. Morphological changes of the Harlingvliet estuary after closure in 1970. *Coast. Eng.* 44 (3), 191–203. [http://dx.doi.org/10.1016/S0378-3839\(01\)00026-6](http://dx.doi.org/10.1016/S0378-3839(01)00026-6), www.elsevier.com/locate/coastaleng <https://linkinghub.elsevier.com/retrieve/pii/S0378383901000266>.
- Tulp, I., Bolle, L., Rijnsdorp, A., 2008. Signals from the shallows: In search of common patterns in long-term trends in dutch estuarine and coastal fish. *J. Sea Res.* 60 (1–2), 54–73. <http://dx.doi.org/10.1016/j.seares.2008.04.004>, <https://linkinghub.elsevier.com/retrieve/pii/S1385110108000348>.
- Van Diggelen, A., Montagna, P., 2016. Is salinity variability a benthic disturbance in estuaries? *Estuaries Coasts* 39 (4), 967–980. <http://dx.doi.org/10.1007/s12237-015-0058-9>, <http://link.springer.com/10.1007/s12237-015-0058-9>.
- Vasiliev, D., 2022. The role of biodiversity in ecosystem resilience. *IOP Conf. Ser.: Earth Environ. Sci.* 1072, 012012. <http://dx.doi.org/10.1088/1755-1315/1072/1/012012>, <https://iopscience.iop.org/article/10.1088/1755-1315/1072/1/012012>.
- van Wesenbeeck, B., Mulder, J., Marchand, M., Reed, D., de Vries, M., de Vriend, H., Herman, P., 2014. Damming deltas: A practice of the past? Towards nature-based flood defenses. *Estuar. Coast. Shelf Sci.* 140, 1–6. <http://dx.doi.org/10.1016/j.ecss.2013.12.031>, <https://linkinghub.elsevier.com/retrieve/pii/S0272771413005556>.
- Whitfield, A., Elliott, M., Basset, A., Blaber, S., West, R., 2012. Paradigms in estuarine ecology - a review of the remane diagram with a suggested revised model for estuaries. *Estuar. Coast. Shelf Sci.* 97, 78–90. <http://dx.doi.org/10.1016/j.ecss.2011.11.026>.
- Worm, B., Barbier, E., Beaumont, N., Duffy, J., Folke, C., Halpern, B., et al., 2006. Impacts of biodiversity loss on ocean ecosystem services. *Science* 314 (5800), 787–790. <http://dx.doi.org/10.1126/science.1132294>, <https://www.science.org/doi/10.1126/science.1137946> <https://www.science.org/doi/10.1126/science.1132294>.
- Yachi, S., Loreau, M., 1999. Biodiversity and ecosystem productivity in a fluctuating environment: The insurance hypothesis. *Proc. Natl. Acad. Sci.* 96 (4), 1463–1468. <http://dx.doi.org/10.1073/pnas.96.4.1463>, www.pnas.org/https://pnas.org/doi/full/10.1073/pnas.96.4.1463.
- Yang, Z., Sobocinski, K., Heatwole, D., Khangaonkar, T., Thom, R., Fuller, R., 2010. Hydrodynamic and ecological assessment of nearshore restoration: A modeling study. *Ecol. Model.* 221 (7), 1043–1053. <http://dx.doi.org/10.1016/j.ecolmodel.2009.07.011>.
- Ye, W., Xu, X., Wang, H., Wang, H., Yang, H., Yang, Z., 2016. Quantitative assessment of resources and environmental carrying capacity in the northwest temperate continental climate ecotone of China. *Environ. Earth Sci.* 75 (10), <http://dx.doi.org/10.1007/S12665-016-5607-4>.
- Ysebaert, T., Herman, P., Meire, P., Craeymeersch, J., Verbeek, H., Heip, C., 2003. Large-scale spatial patterns in estuaries: Estuarine macrobenthic communities in the schelde estuary, NW europe. *Estuar. Coast. Shelf Sci.* 57 (1–2), 335–355. [http://dx.doi.org/10.1016/S0272-7714\(02\)00359-1](http://dx.doi.org/10.1016/S0272-7714(02)00359-1).